Aldose Reductase Deficiency Protects from Autoimmune- and Endotoxin-Induced Uveitis in Mice

Umesh C. S. Yadav, Mohammed Shoeb, Satish K. Srivastava, and Kota V. Ramana

Purpose. To investigate the effect of aldose reductase (AR) deficiency in protecting the chronic experimental autoimmune (EAU) and acute endotoxin-induced uveitis (EIU) in c57BL/6 mice.

Methods. The WT and AR-null (ARKO) mice were immunized with human interphotoreceptor retinoid-binding peptide (hIRPB-1–20), to induce EAU, or were injected subcutaneously with lipopolysaccharide (LPS; 100 μg) to induce EIU. The mice were killed on day 21 for EAU and at 24 hours for EIU, when the disease was at its peak, and the eyes were immediately enucleated for histologic and biochemical studies. Spleen-derived T-lymphocytes were used to study the antigen-specific immune response in vitro and in vivo.

Results. In WT-EAU mice, severe damage to the retinal wall, especially to the photoreceptor layer was observed, corresponding to a pathologic score of ~2, which was significantly prevented in the ARKO or AR inhibitor–treated mice. The levels of cytokines and chemokines increased markedly in the whole-eye homogenates of WT-EAU mice, but not in ARKO-EAU mice. Further, expression of inflammatory marker proteins such as inducible nitric oxide synthase (iNOS), cyclooxygenase (COX)-2, tumor necrosis factor (TNF)-α, and vascular cell adhesion molecule (VCAM)-1 was increased in the WT-EIU mouse eyes but not in the ARKO-EIU eyes. The T cells proliferated vigorously when exposed to the hIRPB antigen in vitro and secreted various cytokines and chemokines, which were significantly inhibited in the T cells isolated from the ARKO mice.

Conclusions. These findings suggest that AR-deficiency/inhibition protects against acute as well as chronic forms of ocular inflammatory complications such as uveitis. (*Invest Ophthalmol Vis Sci.* 2011;52:8076–8085) DOI:10.1167/iovs.11-7830

Uveitis, a common cause of vision loss, accounts for 5% to 15% of all cases of blindness worldwide affecting individuals of all ages, both sexes, and all races.[1] In the United States, a total of 150,000 cases of uveitis are reported annually, and approximately 10% result in severe visual handicaps.[2] In most of the patients, the etiology is difficult to define, as the causes could vary from infections, trauma, and autoimmune diseases, such as rheumatoid arthritis, systemic lupus erythematosus, polyarthritis nodosa, relapsing polychondritis, Wegener's granulomatosis, scleroderma, Behçet's disease, Reiter's disease, Crohn's disease, and ankylosing spondylitis.[1,3–7] Although there is no appropriate animal model for the study of such a varied pathophysiology in humans, the closest to endogenous uveitis in humans are the acute form of bacterial endotoxin, lipopolysaccharide (LPS)-induced uveitis, and experimental autoimmune uveitis (EAU) induced in mice by immunization with retinal antigenic peptides.[8–10] Various investigators have suggested the use of these animal models to study the efficacy of pharmacologic inhibitors in patients.[11,12]

In the past few years, aldose reductase (AR), a rate-limiting enzyme of the polyol pathway that reduces glucose into sorbitol in the presence of reduced nicotinamide adenine dinucleotide phosphate (NADPH), has emerged as the molecular target that mediates various inflammatory diseases.[5,13–15] We have shown that AR mediates the pathogenesis of endotoxin-induced uveitis (EIU) in rats, and its inhibition could be beneficial in the treatment of acute uveitis.[16] Since the pathophysiology of endogenous uveitis differs from that of the exogenous form, particularly infection-induced uveitis, and involves the participation and activation of Th-1 lymphocytes, we have investigated whether genetic deficiency or inhibition of AR could be protective against disease development in a mouse model of uveitis. We have also tested the efficacy of fidarestat, a highly specific inhibitor of AR, against both forms of uveitis. Fidarestat was used because it has already undergone a phase III clinical trial for diabetic neuropathy and was found to be safe for human use.[17]

Besides the different mechanism in the pathophysiology, the common denominator in both types of uveitis is the inflammation that stems from the oxidative stress caused by different stimuli.[18–22] The oxidative stress is generated in the endotoxin-induced uveitis by the bacterial cell wall component, LPS which is known to activate NADPH oxidases (NOX).[23,24] Further, in autoimmune uveitis, oxidative stress emanates from the ongoing systemic chronic inflammation in the body which activates the circulating leukocytes. The activated leukocytes cross the blood–retinal barrier and generate more ROS, thereby severely damaging the photoreceptor layer in the retinal wall and exacerbating the pathophysiology of endogenous uveitis.[25,26] Several investigators have demonstrated that oxidative stress-induced inflammatory process is one of the key contributing factors in the pathophysiology of uveitis.[13,20,27] Therefore, containing the oxidative stress–induced molecular signals that transcribe inflammatory cytokines, chemokines, and other mediators could suppress the inflammation and ameliorate the potentially sight-threatening pathology. Since we and others have demonstrated previously that AR inhibition blocks the molecular signals initiated by oxidative stress and thus prevents several pathologic conditions, including diabetic, cardiovascular, sepsis, cancer, and allergy in animal models,[28–35] we postulate that pharmacological inhibition or genetic silencing of this enzyme could offer a potential opportunity to treat both acute and chronic forms of ocular inflammation in uveitis. Therefore, we investigated the

From the Department of Biochemistry and Molecular Biology, University of Texas Medical Branch, Galveston, Texas.

Supported by National Institutes of Health Grants EY015891 and GM071036 (KVR) and DK36118 (SKS).

Submitted for publication May 5, 2011; revised August 11 and 31, 2011, accepted September 2, 2011.

Disclosure: **U.C.S. Yadav**, None; **M. Shoeb**, None; **S.K. Srivastava**, and **K.V. Ramana**, None

Corresponding author: Kota V. Ramana, 6.614D BSB, Department of Biochemistry and Molecular Biology, University of Texas Medical Branch, Galveston, TX 77555; kvramana@utmb.edu.

effect of AR deficiency as well as the efficacy of the AR inhibitor fidarestat in the prevention of both chronic (i.e., experimental autoimmune [EAU]) and acute endotoxin–induced uveitis (EIU) in mice. Our results showed that AR deficiency prevented the inflammatory changes in mouse eyes associated with EAU and EIU induced by immunization with hIRBP and injection of the bacterial endotoxin LPS, respectively. These findings suggest that AR inhibition could be used in the treatment of ocular inflammatory complications such as uveitis.

Materials and Methods

Materials

Human IRBP-derived peptide 1-20 (H2N-GPTHLFQPSLVLDMAKVLLD-OH) was synthesized and purified by CHI-Scientific (Maynard, MA). Complete Freund's adjuvant (CFA) was purchased from Sigma-Aldrich (St. Louis, MO). Purified *Bordetella pertussis* toxin (PTX) was from Calbiochem (San Diego, CA). *Mycobacterium tuberculosis* H37RA was purchased from Difco Laboratories (Detroit, MA). RPMI-1640 medium, phosphate-buffered saline (PBS), gentamicin sulfate solution, penicillin and streptomycin, trypsin/EDTA (EDTA) solution, and fetal bovine serum (FBS) were purchased from Invitrogen-Gibco (Grand Island, NY). Fidarestat was obtained as a gift from Sanwa Kagaku Kenkyusho Co. Ltd. (Nagoya, Japan). Dimethyl sulfoxide (DMSO) was obtained from Fisher Scientific (Pittsburgh, PA). Antibodies against iNOS, COX-2, and VCAM-1 were from Santa Cruz Biotechnology, Inc. (Santa Cruz, CA) and TNF-α antibodies were purchased from Abcam (Cambridge, MA). A membrane-based cytokine array system was purchased from RayBiotech, Inc. (Norcross GA). All other reagents used were of analytical grade.

Animals

Approximately 8-week-old C57BL/6 mice were obtained from Harlan Laboratories (Indianapolis, IN), and AR-knockout (ARKO) mice were bred and maintained in a pathogen-free condition in the animal resource center under the 12-hour light and dark cycles, at University of Texas Medical Branch at Galveston, where food and water were provided ad libitum. All studies were conducted in compliance with the ARVO Statement for the Use of Animals in Ophthalmic and Vision Research.

Induction of EAU and EIU

To induce experimental autoimmune uveitis, the mice were immunized by subcutaneous (SC) injections into both hind thighs with 100 μg of hIRBP in 100 μL of emulsion with CFA (1:1, vol/vol), which was supplemented with 2.5 mg/mL of heat-killed *M. tuberculosis* H37Ra (Difco Laboratories), Concurrently, an intraperitoneal (IP) injection containing 0.5 μg purified *B. pertussis* toxin (PTX; Calbiochem) in 100 μL phosphate-buffered saline (PBS) was also administered as an additional adjuvant. For the induction of adoptively transferred uveitis, T cells were isolated from spleen (as described below) of wild-type [WT] and ARKO mice immunized with hIRBP-20 on day 12 after immunization and cultured with 20 mg/mL of IRBP1–20, along with gamma irradiated (2500 rad) syngeneic spleen cells as APCs for 3 days. The activated T cells were separated on a single-density gradient (Ficoll; GE Healthcare, Piscataway, NJ) and 5×10^6 cells suspended in 0.2 mL of PBS were injected per mouse, such that activated T cells from WT mice were injected into WT as well as ARKO mice and that from ARKO mice were injected in WT as well as ARKO mice. The disease severity and histopathologic assessments were performed on day 14 after transfer. EIU was induced in mice by giving SC injection of LPS (100 μg) dissolved in PBS.

AR Inhibitor Treatment

For the treatment of EAU mice from the second day onward, the mice were injected (IP) with the AR inhibitor fidarestat (7 mg/kg/d) in a volume of 25 μL DMSO daily. At this dose, fidarestat significantly inhibited the AR activity (data not shown). The control mice received an equivalent amount of the carrier. For EIU experiments, the mice were treated with the inhibitor 1 day and 2 hours before LPS injection. To examine the therapeutic efficacy of fidarestat, the inhibitor was administered starting on day 12 in drinking water ad libitum, such that they received approximately 150 μg per mouse per day (determined by us based on average water consumption per mouse per day).

Pathologic Assessment of Uveitis in Mice

The severity of EAU and inflammation was scored on a scale of 0 to 4 by slit lamp biomicroscopic examination by an expert ophthalmologist who was blinded to the experimental groups. The scale was as follows: grade 0, no disease, with eyes translucent and reflecting light (red reflex); grade 1, enlargement of the iris vessel and abnormal pupil contraction; grade 2, cellular infiltrates and hazy anterior chamber, with a decreased red reflex; grade 3, a moderately opaque anterior chamber, with the pupil still visible and a dull red reflex; and grade 4, an opaque anterior chamber, obscured pupil, and absence of red reflex.[36]

Histology

The mice were killed on day 21, when maximum disease activity was reported. The eyes were enucleated and either quickly frozen for biochemical determinations later or fixed in special solution for 24 hours, followed by dehydration, paraffin embedding, and sectioning (5 μm) for histopathologic examination, after staining with hematoxylin and eosin (H&E). For histopathologic evaluation, the iris-ciliary body complex, anterior chamber, vitreous, and retina were observed under light microscope. The spleens were harvested immediately and used for the separation of T cells which were used in the antigen-induced cell-viability assay and for the determination of levels of inflammatory cytokines and chemokines, as described below.

Immunohistochemical Studies

The paraffin-embedded sections were deparaffinized by warming at 60°C for 1 hour and incubation in xylene three times for 10 minutes each followed by rehydration by passing through 100%, 95%, 80%, and 70% ethanol and finally deionized water. The sections were rinsed in PBS two times for 5 minutes each and incubated with blocking buffer (2% BSA, 0.1% Triton X-100, 2% normal rabbit IgG, and 2% normal goat serum) overnight at 4°C. They were then incubated with antibodies against iNOS (1:250 dilution), COX-2 (1:300 dilution) overnight at 4°C. The sections were incubated with fluorescein isothiocyanate (FITC)–labeled secondary antibodies. The slides were mounted with mounting medium containing fluorescent 4′,6-diamidino-2-phenylindole (DAPI; Vectashield; Vector Laboratories, Burlingame, CA) and examined under a fluorescence (using FITC filters) microscope (EPI-800 microscope; Nikon, Tokyo, Japan) and photographed with a digital camera fitted to the microscope.

T-Cell Viability Assay Using the MTS Assay

The T-cell viability assay in response to the antigen (hIRBP peptide) was performed with spleen-derived T lymphocytes. The splenocytes were obtained from mouse spleens (gentleMACS Dissociator; Miltenyi Biotec, Auburn, CA), and T-cell-enriched fractions were prepared by passing the dispersed splenocytes over nylon-wool columns. Nylon-wool nonadherent cells (2×10^5/well) were cultured in quadruplet with gamma-irradiated (2500 rad) syngeneic spleen cells and 20 μg of peptide in a 96-well flat-bottomed microtiter plate for 72 hours at 37°C. The T-cell viability measured by a nonradioactive cell-proliferation assay using MTS dye (CellTiter 96 AQ_{ueous}; Promega; Madison, WI), composed of solutions of tetrazolium compound (3-(4,5-dimethylthiazol-2-yl)-5-(3-carboxymethoxyphenyl)-2-(4-sulfophenyl)-2H-tetrazolium). At the end of incubation, the MTS dye was added in the wells and incubated for an additional 3 hours, and the plates were read at 490 nm

with a multiwell ELISA plate reader. The absorbance represented T-cell growth in response to antigen, and the data are presented as the mean absorbance ± SD.

Determination of IL-17 Levels in T-Cell Culture Media

To assess the antigen-specific immune response of T-lymphocytes in vitro, IL-17 cytokine produced in the T-cell culture supernatant was quantified. The spleen-derived T cells (5×10^5/well) were cultured with 20 μg hIRBP in the absence or presence of fidarestat (10 μM; dissolved in water) for 72 hours. The control cells received equivalent volumes of carrier. At the end of incubation, the culture media were harvested, cleared by centrifugation (5000 rpm; 5 minutes), and stored at −80°C until used for the IL-17 determinations using a mouse cytokine antibody array system, according to the manufacturer's instructions (Cosmo Bio, Carlsbad, CA).

Determination of Inflammatory Cytokines Levels in T-Cell Culture Media and Whole Eye Lysate

The T-cell media were obtained, as described above, and whole-eye lysates were prepared by homogenizing the eyeballs in RIPA lysis buffer, containing protease inhibitor cocktail. Inflammatory cytokines and the chemokine profile in T-cell culture media and whole-eye homogenates were determined with a mouse cytokine antibody array system (RayBio, Norcross, GA) that determines the expression of 64 inflammatory markers from a single sample, according to the manufacturer's instructions. The culture media and tissue homogenates were incubated with an antibody array support membrane; the membrane was specifically coated with various antigens to capture an array of cytokines and chemokines. The tagged proteins were detected by conjugation with biotinylated antibodies and a streptavidin system. The fold change was calculated from the measured intensities of the individual spots signal developed on x-ray film using densitometry software (Eastman Kodak, Rochester, NY).

Western Blot Analysis

The whole-eye lysate was prepared by homogenizing the eyeballs in ice-cold RIPA lysis buffer containing 1 mM dithiothreitol, 1 mM phenylmethylsulfonyl fluoride, and 1:100 dilutions of protease inhibitor and phosphatase inhibitor cocktails (Sigma-Aldrich) on ice. The whole-eye lysates were cleared by centrifugation at 12,000*g* for 10 minutes at 4°C. The amount of protein in the lysates was determined using the Bradford reagent (Bio-Rad Laboratories, Hercules, CA). Western blot analysis was performed as described by us elsewhere,[30] using antibodies against iNOS, COX-2, VCAM-1, TNF-α, phospho-PKC βII, PKC βII, phospho-p65, and p65, and the membranes were reprobed using antibodies against the housekeeping protein glyceraldehyde 3-phosphate dehydrogenase (GAPDH) to assess the equal loading of proteins.

Statistical Analysis

The data are presented as the mean ± SD, and *P* values were determined by unpaired Student's *t*-test. For animal studies, data collected from in vitro and in vivo experiments were analyzed by ANOVA, followed by Bonferroni post hoc analyses for least significant difference, and $P < 0.05$ was considered statistically significant.

Results

Histopathology of EAU

We determined the effect of AR deficiency on the pathophysiology of EAU by examining the clinical score of the disease on day 21 when the disease was at its peak. As shown in Figure 1A, the WT mice with EAU had a significantly high ($P < 0.001$) pathologic score of 3.12 ± 0.41 on the scale of 4 and the ARKO mice had an average score of 1.38 ± 0.48 which was significantly ($P < 0.02$) less than the pathologic score in the WT EAU mice. When histopathologic symptoms of the two groups were compared, the sections of the WT EAU eyes showed inflammatory cell infiltration in the posterior as well as anterior chambers, accompanied with the blebbing and extensive damage of the photoreceptor layer in the retina (Fig. 1B). These changes were markedly absent in the ARKO mice, except that in one third of the mice with EAU, mild cellular infiltration, retinal edema, and damage to photoreceptor layers were observed, suggesting that the deficiency of AR protected the development of EAU on immunization with the antigen.

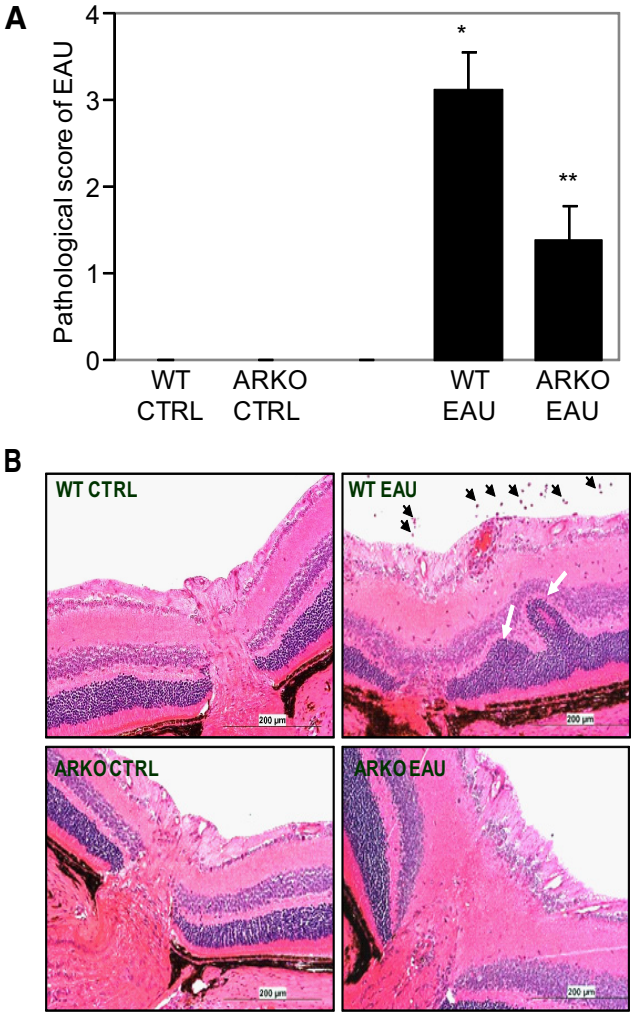

Figure 1. AR deficiency protects the retinal wall (photoreceptor layer) in hIRBP-induced EAU in the mouse eye. (**A**) Pathologic assessment of EAU in WT and ARKO mice was performed by an expert ophthalmologist using a slit lamp microscope, and the eyes were graded on the scale of 0 (normal eye) through 4 (severe uveitis) on day 21 after immunization with hIRBP. The results are expressed as the mean ± SD ($n = 6$), *$P < 0.001$ vs. WT CTRL; **$P < 0.01$ vs. WT EAU. (**B**) The paraffin-embedded sections were stained with hematoxylin and eosin and observed under a light microscope. A representative photomicrograph from each group is shown ($n = 6$). *Black arrows*: infiltrating leukocytes; *white arrows*: damaged photoreceptor layer. CTRL, control. Original magnification, ×200.

Adoptive Transfer of Antigen-Activated T Cells Derived from AR-Null Mice Does Not Induce EAU

Next, we examined the effect of AR deficiency on the EAU caused by adoptive transfer of activated T cells where $CD4^+$ T cells were isolated from the hIRBP-immunized WT and ARKO

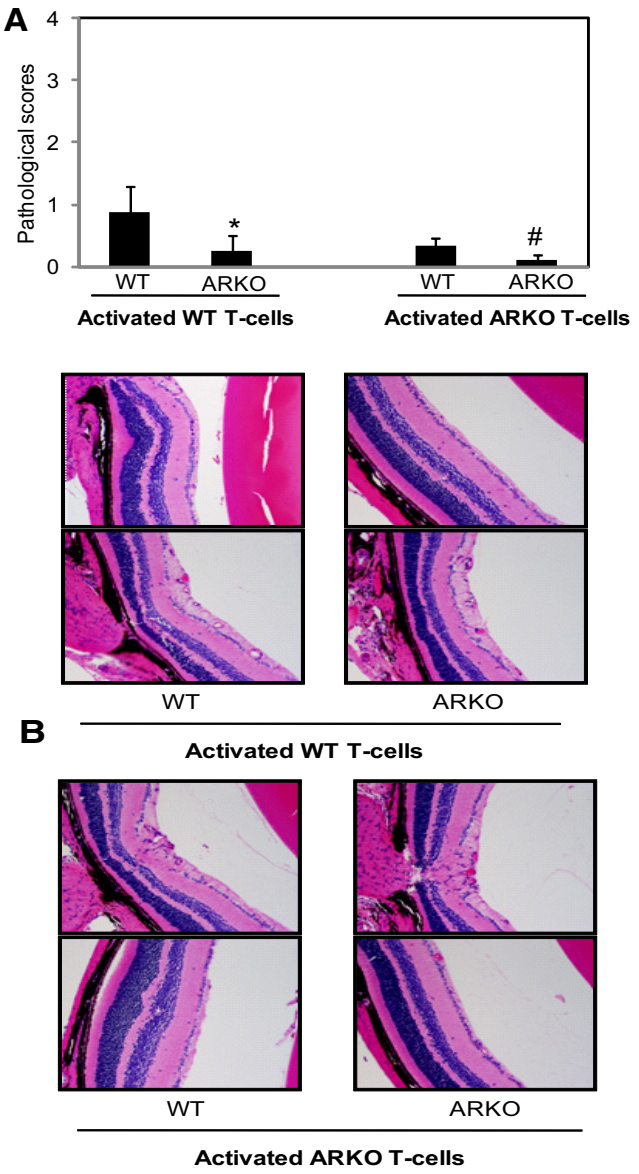

FIGURE 2. Adoptive transfer of antigen-activated T cells derived from AR-null mice fail to induce EAU. Spleen-derived T cells from hIRBP-immunized WT and ARKO mice were activated in the presence of γ-irradiated syngenic APCs and antigen (hIRBP, 20 μg/mL) and the same number of activated T cells were adoptively transferred into WT and ARKO mice. (**A**) The bars shown pathologic score (mean ± SD; $n = 4$) at day 14 after transfer of T cells. $^*P < 0.05$ vs. WT injected with WT T cells; $\#P < 0.05$ vs. WT mice injected with ARKO T cells (**B**) The hematoxylin and eosin–stained eye sections were observed under light microscope and photographed on a camera-equipped fluorescence microscope. A representative photomicrograph from two different animals is shown ($n = 4$). CTRL, control. Original magnifications, ×200.

mice on day 12 and activated in the presence of γ-irradiated syngenic APCs and antigen (hIRBP, 20 μg/mL) and WT T cells, and the same number of antigen-activated and expanded T-cells from WT and ARKO mice were adoptively transferred into both WT and ARKO mice. As presented in Figure 2, WT T cells caused disease of moderate severity (histopathologic score, 0.875 ± 0.22) in the WT mice, whereas in the ARKO mice, the disease was very mild (histopathologic score, 0.25 ± 0.05). When antigen-activated T cells from the ARKO mice were transferred to the WT or the ARKO mice, no disease was observed in either the WT or the ARKO mice (Fig. 2). These results indicate that protection offered by AR deficiency is most likely due to nonactivation and lack of expansion of the pathologic subsets of T cells.

Viability of Spleen-Derived T Cells after Stimulation with hIRBP

To confirm whether protection by AR deficiency is due to nonactivation and lack of expansion of the pathologic T-cell subset, we next measured the viability of spleen-derived T cells in response to antigen hIRBP. We isolated T cells from mouse spleen and purified them over nylon-wool columns and, as determined by fluorescence-activated cell sorting (FACS) analysis, the T-cell population was more than 95% pure (data not shown). The WT EAU mouse–derived T-cell population increased more than twofold compared with T cells derived from WT control mice when incubated for 72 hours in the culture media alone and further increased to more than fourfold in the presence of antigen. On the other hand, the viability of T cells from the ARKO EAU mice was significantly lower, approximately 50% less in the absence of antigen and more than 85% less when the antigen was present in the culture medium compared with WT EAU (Fig. 3). T cells derived from the control did not grow in the absence or the presence of antigen. These results suggest that AR regulates the antigen-induced growth of primed T cells and its absence was crucial in slowing the viability of spleen-derived T cells.

Expression of the Inflammatory Markers iNOS and COX-2 during EAU

Next, we immunostained the eye sections with antibodies for the inflammatory marker iNOS and COX-2, which are well-known participants in the inflammation during uveitis. As shown in Figure 4A, there was a marked increase in the expression of iNOS in the cells of the retinal wall in the WT mice with EAU, whereas in the ARKO mouse eyes with EAU, iNOS-specific staining was minimal. Similarly, COX-2 expression increased in the retina at day 21 of immunization in the WT mice, as determined by increased fluorescence, whereas in the ARKO mice, the expression was comparatively less and was similar to that in the control mice (Fig. 4B). These

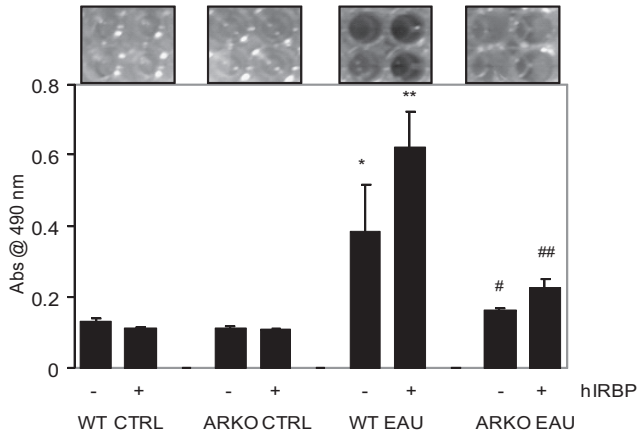

FIGURE 3. AR deficiency suppresses antigen-induced viability of spleen-derived T cells ex situ. The nylon-wool–purified spleen T cells from different groups were incubated with hIRBP for 72 hours and the growth of cultured cells was measured. The data, average absorbance at 490 nm, are expressed as the mean ± SD ($n = 5$; $^*P < 0.01$ vs. WT CTRL-hIRBP; $^{**}P < 0.001$ vs. WT CTRL+hIRBP; $\#P < 0.01$ vs. WT EAU-hIRBP; $\#\#P < 0.001$ vs. WT EAU+hIRBP). CTRL, control.

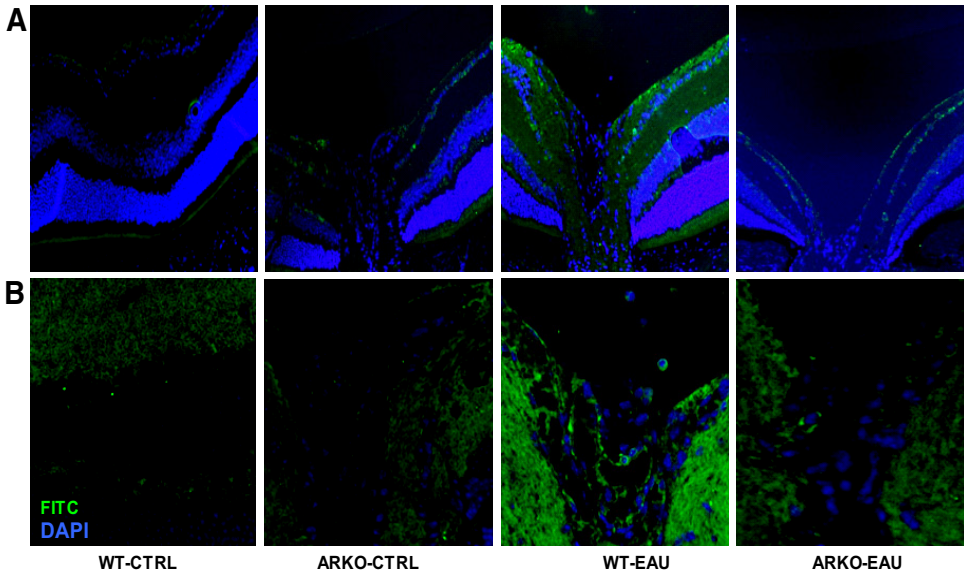

FIGURE 4. AR deficiency suppresses the hIRBP-induced expression of iNOS and COX-2 in mouse ocular tissues. Serial sections of paraformaldehyde-fixed mouse eyes were immunostained with antibodies against (**A**) iNOS and (**B**) COX-2. The antigen-specific fluorescence intensity was observed by fluorescence microscopy. Representative images are shown ($n = 4$). CTRL, control. Original magnification, ×200.

results suggest that EAU-related expression of inflammatory marker proteins was markedly decreased in the ARKO mice.

Inflammatory Cytokine and Chemokine Secretion by Spleen-Derived T Cells after Stimulation with hIRBP

To further assess the role of T cells in inflammation during EAU, we determined the inflammatory markers secreted by T cells in the medium when stimulated with the antigen. As shown in Table 1, the culture media from the WT EAU mouse–derived T cells incubated with hIRBP showed severalfold increased expression of cytokines (such as IL-1α, IL-1β, IL-6, IFN-γ, TNF-α, and IL10) and chemokines (CINC-3, CNTF, Fractalkine, MIP-3α, and MCP1) when stimulated with the antigen, and their levels were comparatively low in the ARKO mice, suggesting that AR deficiency resulted in lower expression of inflammatory markers when challenged with the antigen. The levels of inflammatory markers remained at the basal level (no significant change) in the media of the WT and ARKO-derived T cells with no antigen challenge.

Secretion of IL-17 by Spleen-Derived T Cells after Stimulation with hIRBP

Since IL-17 has been implicated in the pathogenesis of EAU,[37–38] we next measured the levels of IL-17 in the T-cell culture media 72 hours after hIRBP challenge. As shown in Figure 5, the T-cell media from the control animals had only a basal level of IL-17, as did the media from unchallenged T cells from the EAU WT and ARKO mice. When challenged with hIRBP, the levels of IL-17 increased significantly to 424 ± 45 pg/mL in the EAU-derived T-cell media which was approximately 20 pg/mL without hIRBP challenge and was 203 ± 33.8 pg/mL (~50% less compared with the WT EAU) in the ARKO group treated with hIRBP. These results suggest that IL-17 is elevated in T-cell culture medium, a subpopulation of Th-17

TABLE 1. Expression of Inflammatory Markers in Culture Media from EAU Mouse–Derived T Cells Incubated with hIRBP

Growth Factors, Cytokines, Chemokines	Fold Change
WT-EAU vs. ARKO-EAU	
CINC-3, CNTF, Fractalkine, GM-CSF, IFN-γ, IL-1α, IL-1β, IL-6, IL-10, Leptin, MCP-1, MIP-3α, β-NGF, TIMP-1, TNF-α, VEGF	0–1
WT-EAU vs. WT-EAU+IRBP	
CINC-3, CNTF, Fractalkine, IL-6, MIP-3α,	2–5
IFN-γ, IL-1α, IL-1β, IL-10, Leptin	1–3
GM-CSF, β-NGF, TNF-α, VEGF	2–5
TIMP-1, MCP-1	5–6
ARKO-EAU+IRBP vs. WT-EAU+IRBP	
CINC-3, Fractalkine, IL-4, IL-6, IL-10, CINC-2, CTNF, IFN-γ, IL-1α, IL-1β, LIX, Leptin, MIP-3α, β-NGF	0–1
MCP-1, TIMP-1, TNF-α, VEGF	1–2

AR deficiency prevented an hIRBP-induced increase in cytokines, chemokines, and growth factors in spleen-derived T-cell culture media. A membrane-based cytokine antibody array system was used to determine the expression levels of the inflammatory factors in the T-cell media. The spots on the array-membrane were analyzed by densitometry and the data are presented as fold change in expression. The WT-EAU and ARKO EAU T-cell media served as the controls ($n = 4$).

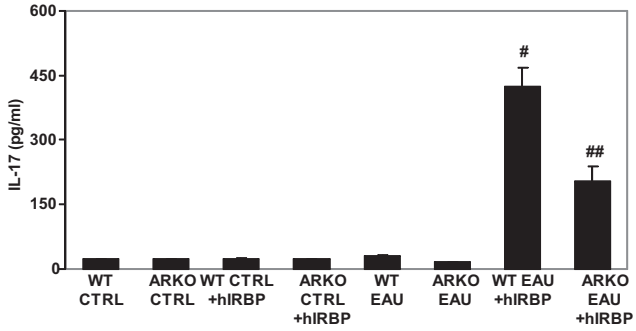

FIGURE 5. AR deficiency reduces hIRBP-induced IL-17 release by spleen-derived T cells. The nylon-wool–purified, spleen-derived T cells from different groups were incubated with hIRBP for 72 hours. The culture media supernatants were used for the determination of IL-17 by an ELISA. Data are expressed as the mean ± SD ($n = 5$; #$P < 0.001$ vs. WT EAU; ##$P < 0.01$ vs. WT EAU+hIRBP). CTRL, control.

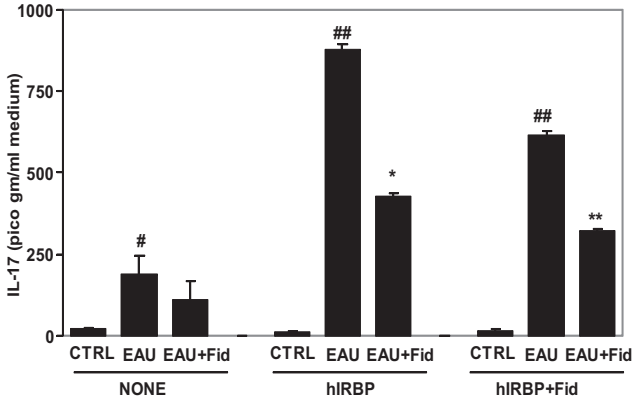

FIGURE 7. AR inhibition prevents hIRBP-induced IL-17 release from T cells. The T cells isolated from control, EAU, and EAU+Fid mouse spleens and purified using nylon-wool columns were incubated with hIRBP for 72 hours. The culture media supernatants were collected and used for the determination of IL-17 by ELISA. The results are expressed as the mean ± SD ($n = 5$). (#$P < 0.01$ vs. CTRL; ##$P < 0.0003$ vs. CTRL+hIRBP; *$P < 0.001$ vs. EAU+hIRBP; ##$P < 0.001$ vs. CTRL+hIRBP+Fid; **$P < 0.01$ vs. EAU+IRBP+Fid. CTRL, control; Fid, fidarestat.

cells differentiate in the spleen-derived T cells when challenged with antigen, and AR plays a critical role in this process.

AR Inhibition by Fidarestat Prevents Pathogenesis of EAU in Mouse Eyes

Next, we used a specific AR inhibitor, fidarestat, and examined the pathogenesis of EAU. As shown in Figure 6A, the clinical EAU score of 3 in the WT mice was decreased by ~50% when the mice were treated with fidarestat. Further, when fidarestat was administered to the mice after the disease had established, on day 12 after immunization, there was a significant (>70%) decrease in the pathologic score of the disease compared with the group that was not administered the drug (Figs. 6B, 6C), indicating the therapeutic efficiency of AR inhibition.

We further measured T-cell viability in the presence of antigen hIRBP, without or with fidarestat, and observed that in the absence of AR inhibitor, the T cells proliferated approximately two-fold, whereas in the presence of inhibitor, their number did not increase significantly (data no shown). We further measured the levels of IL-17 in the T-cell media after antigen challenge. As shown in Figure 7, in the absence of hIRBP, the level of IL-17 increased significantly in the EAU-derived T-cell media compared with that of the control T cells, and T cells derived from fidarestat-treated mice showed significantly decreased IL-17 levels. However, when stimulated with the hIRBP, the EAU-derived T cells produced a significantly increased IL-17 in the culture media compared with control T cells. In T-cell medium from the fidarestat-treated EIU mice, the level of IL-17 was significantly lower than in the EAU-derived T-cell medium. Furthermore, when the T cells were stimulated with the hIRBP in the presence of the AR inhibitor, the EAU-

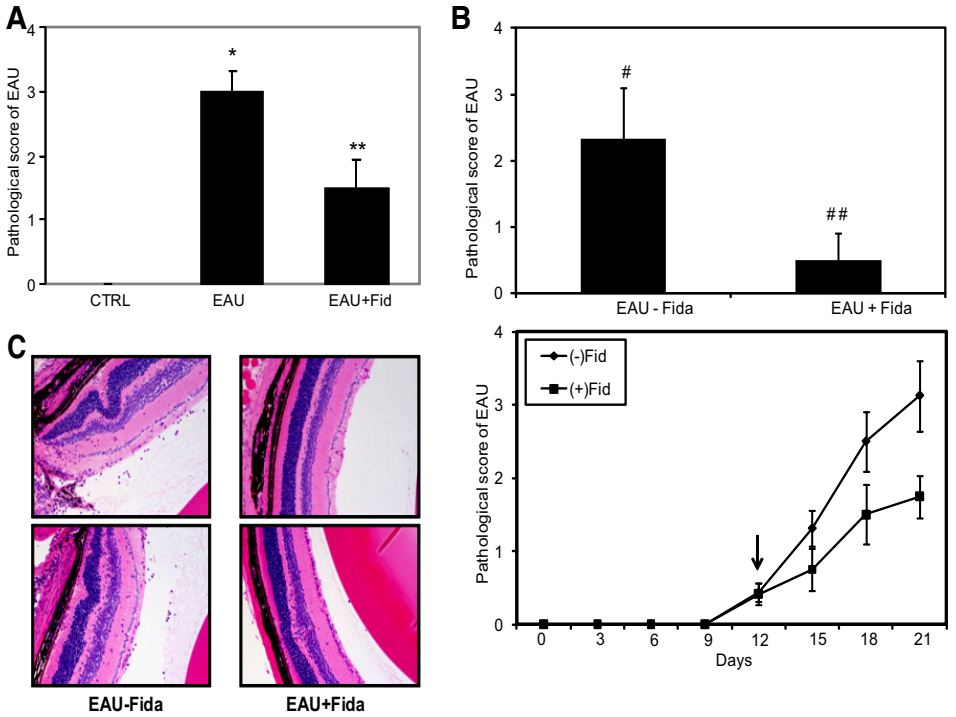

FIGURE 6. AR inhibition ameliorates hIRBP-induced EAU in mouse eyes. The AR inhibitor fidarestat was administered to the mice, either (**A**) 2 days or (**B**) 12 days after immunization with hIRBP. The eyes were examined using slit lamp microscope and pathologic score was determined. The bar graph shows pathologic score at the end of the experiment and line graph shows pathologic scores with time. The results are expressed as the mean ± SD ($n = 4$–6; *$P < 0.001$ vs. control; **$P < 0.001$ vs. EAU+Fid; #$P < 0.01$ vs. EAU-Fid; ##$P < 0.001$ vs. EAU+Fid. *Arrow*: start of fidarestat administration. (**C**) The eyes from (**B**) were fixed and paraffin embedded, and 5-μm-thin sections were stained with hematoxylin and eosin and observed under light microscope. A representative photomicrograph of two different animals is shown ($n = 4$). CTRL, control; Fid, fidarestat. Original magnification, ×200.

derived T cells still produced a significantly increased IL-17 in the culture medium, whereas in T-cell medium from the fidarestat-treated EIU mice, the level of IL-17 was significantly reduced compared with that in medium from the EAU-derived T cells.

AR Deficiency in Mice Protects against the Acute Form of Uveitis

After determining the role of AR in the chronic form of uveitis in mice, we examined the role of AR deficiency in the acute form of uveitis in ARKO mice. As shown in Figure 8A, the clinical score of the disease was 2.41 ± 0.64 in the WT mice at 24 hours after LPS injection, whereas in the ARKO mice, the clinical score decreased significantly (~50%) and was 0.98 ± 0.40.

Since the aqueous humor from the mouse eye is in miniscule amounts and is difficult to obtain, we used whole-eye lysate to determine the inflammatory markers in the eye. As shown in Table 2, the levels of inflammatory cytokines and chemokines increased significantly in the WT EIU mouse eye whereas in the ARKO EIU mice, their levels were markedly less.

We further examined the expression of other inflammatory markers in eye lysate such as TNF-α, iNOS, COX-2, and VCAM-1, which were found to be elevated several fold in eyes from the EIU WT mice, whereas their expression level was significantly less in the ARKO EIU mouse eye (Fig. 8B). The control mouse eye had basal levels of expression of these inflammatory proteins. We next examined the activation of signaling molecule PKC and transcription factor nuclear factor-κB (NF-κB), the key mediators of redox signals, in the whole-eye lysate. At 24 hours after the LPS injections, there was increased phosphorylation of PKC βII and NF-κB in the whole-eye lysate from the WT EIU mice, whereas in the ARKO EIU mouse eye lysates, phosphorylation was similar to the basal levels in the control mouse eyes lysates (Fig. 8C). Taken together, these results thus suggest that deficiency of AR offers protection in acute form of exogenous uveitis which is caused mainly by infection.

Discussion

In the present study, we have investigated the effect of AR deficiency and efficacy of the AR inhibitor fidarestat in chronic (EAU) and acute (EIU) models of mice immunized with hIRBP or injected with the bacterial endotoxin LPS. Our results show that whereas the WT mice exhibited a severe onset of disease at day 21 after hIRBP immunization or 24 hours after LPS injections, the ARKO mice showed significantly fewer symptoms associated with EAU or EIU pathogenesis. In both models of uveitis, the ARKO mice showed significant prevention of the disease.

We have demonstrated that pharmacologic inhibition of AR significantly prevents LPS-induced uveitis in rats by blocking the ROS–induced signaling that activates NF-κB.[16] However, to confirm the involvement of AR in the pathogenesis of uveitis, we considered it necessary to use an AR-knockout experimental animal model, and since generating such model is not possible in rats, we used ARKO mice on the C57BL/6 background for our studies. These mice had mild impairment in water reabsorption in the kidney, leading to slightly increased urine output and increased water consumption, but had no phenotypic alteration in the eye.[39]

The pathogenesis of EAU in mice presents an enormous similarity with the posterior uveitis in humans with autoimmune etiology.[10,11] The immunization with a retinal peptide, such as hIRBP, with concurrent administration of PTX and CFA containing heat-killed tuberculosis bacteria triggers bacterial pattern recognition receptors on immune cells, such as monocytes, dendritic cells, neutrophils, natural killer (NK) cells, and T cells and provides the proinflammatory environment that activates the autopathogenic effector pathway leading to uveitis pathogenesis.[12] This model of uveitis is not only similar to the human endogenous uveitis in terms of the clinical symptoms, but it also shares the basic pathogenic mechanism.[10–12] Similarly, the bacterial endotoxin-induced uveitis is used to investigate the mechanism and therapeutic intervention of anterior uveitis in humans.[8,40] Further, the role of oxidative stress in the pathogenesis of uveitis has been recognized in both forms of the disease.[19,20,27,28,41,42] Recently, investigators have identified mitochondrial oxidative stress in the photoreceptor layer during early EAU, which apparently resulted from

Table 2. Expression of Inflammatory Markers in Culture Media from EIU Mouse–Derived T-Cells Injected with Lipopolysaccharide

Growth Factors, Cytokines, Chemokines	Fold Change
WT-CTRL vs. ARKO CTRL	
VEGF, Fractalkine, GM-CSF, IFN-γ, Leptin, MCP-1, MIP-3α, β-NGF, TIMP-1, IL-1α, IL-1β, IL-6, IL-10, TNF-α, CINC-3, CNTF	0–1
WT-EIU vs. WT-CTRL	
CINC-3, CNTF, Fractalkine, IL-6, MIP-3α,	0–1
IFN-γ, IL-1α, IL-1β, IL-10, Leptin, GM-CSF,	1–3
β-NGF, TNF-α, VEGF	2–4
MCP-1, LIX	2–5
TIMP-1	3–5
WT-EIU vs. ARKO-EIU	
IL-4, IL-6, IL-10, CINC-3, Fractalkine, IL-1α, IL-1β, LIX, Leptin, CINC-2, CTNF, IFN-γ, MIP-3α, β-NGF	0–1
VEGF, TIMP-1, TNF-α, MCP-1,	1–2

AR deficiency prevented an LPS-induced increase in cytokines, chemokines, and growth factors in mouse eyes. A membrane-based cytokine antibody array system was used to determine the expression levels of the inflammatory factors in the T-cell media. The spots on the array membrane were analyzed by densitometry, and the data are presented as fold change. The WT-EIU and ARKO-EAU T-cell media served as controls ($n = 4$).

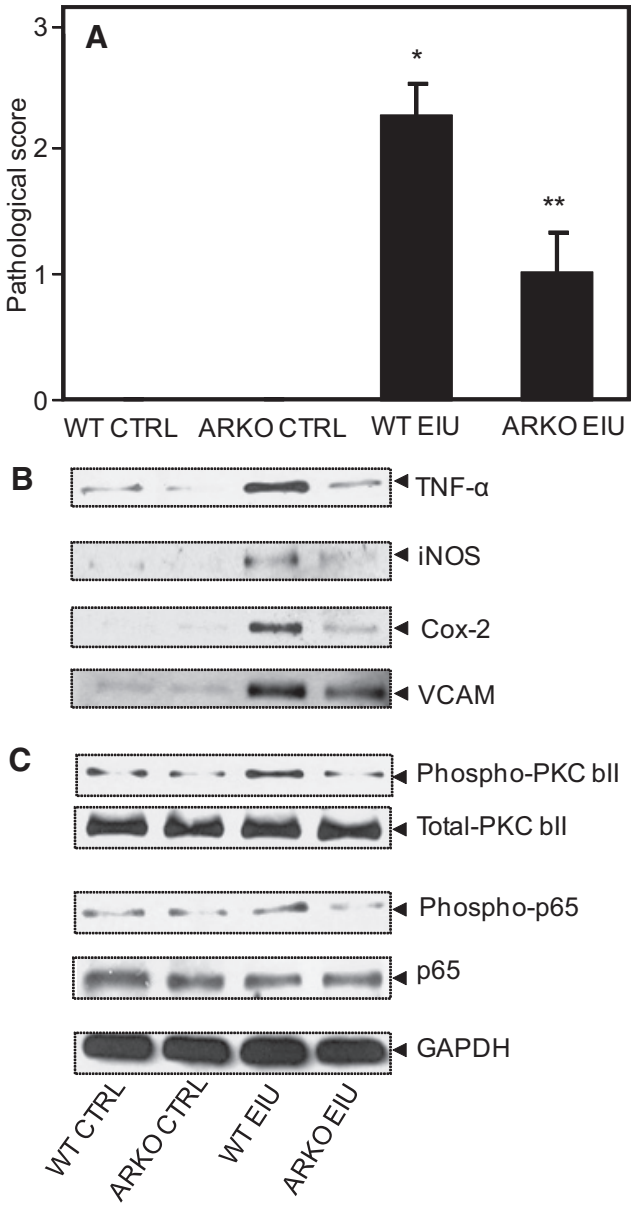

FIGURE 8. AR inhibition prevents EIU-induced expression and activation of various proteins. (**A**) The mouse eyes were examined using a slit lamp microscope and the pathologic score was determined. The results are expressed as the mean ± SD ($n = 4–6$; $^{*}P < 0.001$ vs. WT control; $^{**}P < 0.001$ vs. WT EIU). The whole eye lysates were prepared 24 hours after LPS injections, and an equal amount of proteins from the cleared lysate was used for Western blot analysis by using antibodies against (**B**) TNF-α, iNOS, COX-2, VCAM-1, and GAPDH (**C**) p-PKC βII, PKC βII, P-p50–65, and p65. The blots were stripped and reprobed with antibodies against GAPDH. Representative blots are shown ($n = 4–6$). CTRL, control.

iNOS upregulation in the photoreceptor mitochondria and cytokine generation in the retina by antigen-specific infiltrating T cells.[27] Satici et al.[18] demonstrated increased free radicals in the aqueous humor of an EIU rabbit model and implicated oxygen free radicals in the mediation of inflammation in endotoxin-induced uveitis. For a greater understanding of the role of oxidative stress in the pathogenesis of uveitis and the emerging role of antioxidants in its protection, please refer to our review.[22]

In the present study, we used both models of uveitis (EAU and EIU) in mice to investigate the involvement of AR by using AR deficiency in ARKO mice and also tested the efficacy of a very potent and clinically safe AR inhibitor, fidarestat. Administration of fidarestat had both preventive and therapeutic effects against EAU in mice. We demonstrated earlier that AR mediates the oxidative stress signal in various pathogenic models including diabetes, cancer and metastasis, sepsis, allergic asthma, and uveitis.[13,16,31,33,35] Inhibition of AR blocks the downstream ROS signals and thereby prevents the subsequent activation of signaling cascade that activates redox-sensitive transcription factors, such as NF-κB and activator protein (AP)-1 and transcribe an array of inflammatory markers and cause pathogenesis.[13] We found that in the ARKO mice the EAU was prevented significantly, as the infiltration of inflammatory cells in vitreous and damage to the photoreceptor layer was minimal or absent. Further, the expression of inflammatory enzymes iNOS and COX-2 was comparatively less in the retina of ARKO mice compared with WT mice with EAU.

Since EAU is a T-cell-mediated disease that involves primarily the production of Th1 cytokines by the infiltrating T-lymphocytes, such as IFN-γ, TNF-α, IL-1β, and other cytokines,[43–45] decreased production of Th1 cytokines and chemokines by spleen-derived T cells from ARKO mice in culture suggests that polarized differentiation of naïve T-helper cells into Th1 type was prevented by inhibition of AR. This is highly likely, as JNK and p38 MAP kinases, which are known to activate NF-κB and AP-1 transcription factors, play crucial role in the Th1 polarization of $CD4^+$ cells,[46,47] are also regulated by AR-mediated redox signals.[13,15] We next investigated the effect of adoptive transfer of antigen-activated T cells derived from hIRBP-immunized WT and ARKO mice into both WT and ARKO mice. Our results indicate that, although WT-derived T cells caused disease in WT as well as ARKO mice (though significantly less in ARKO mice), that from ARKO failed to induce disease in either group. These results indicate that protection offered by AR deficiency is most likely due to nonactivation and lack of expansion of the pathologic subsets of T cells. Further, although there was a significant increase in the viability of spleen-derived T cells from WT EAU mice when exposed to the antigen hIRBP in culture, it was significantly less in ARKO mouse spleen–derived T cells. These observations suggest that there is a lack of expansion of the Th1- polarized population and production of Th1 cytokines in ARKO mice and indicate that these events could be regulated by AR.

Some studies have implicated Th-17 in the pathogenesis of uveitis[37,38]; hence, we determined the levels of IL-17, in both conditions (i.e., AR deficiency and pharmacologic inhibition of AR by fidarestat), in the spleen-derived T-cell culture media after incubation with hIRBP for 72 hours. Our results show that T cells derived from EAU mice released increased amounts of IL-17 on stimulation with hIRBP in culture, which significantly decreased in the media of T cells derived from ARKO mice or fidarestat-treated mice, although it remained elevated compared with their respective controls. These results suggest that AR regulates the polarization of $CD4^+$ cells into a population of IL-17 secreting cells and also that AR deficiency or inhibition could prevent the secretion of IL-17 from this population.

We further investigated the effect of AR deficiency in the acute form of the disease by using an EIU model in mice. We injected LPS SC into mice, which caused severe inflammation in the eye, equivalent to a pathologic score more than 2.5 on a scale of 4 in the WT mice which was significantly less in the ARKO mice (~1). Similarly, the levels of various cytokines and chemokines were markedly increased in the eyes of the WT EIU mice, whereas in the ARKO mice, the increase was markedly less. Further, expression of inflammatory marker proteins, such as iNOS, COX-2, TNF-α, and VCAM-1, was increased in the WT EIU mouse eyes, but there was no such increase in the ARKO mice. These results suggest that AR deficiency protects

mice against the pathogenesis of both type of disease (i.e., infection- and autoimmune-induced).

We next tested the effect of AR inhibition and found that administration of fidarestat prevented the development of EIU in mice, as well as the secretion of IL-17 from the T cells isolated from the spleen. These results confirm our findings in the ARKO mice and suggest that AR inhibition could be a novel approach for therapeutic intervention in the management of autoimmune uveitis in humans.

The mechanistic details of how AR regulates the redox signaling are not clear yet. However, the evidence collected in our laboratory in the past decade indicates that oxidative stress generates large amount of lipid-derived aldehydes by peroxidation of membrane lipids, which readily conjugate with glutathione and are reduced to respective alcohols by AR. The reduced GS-lipid alcohols act as signaling intermediates and activate several protein kinases by a still uncertain mechanism, eventually activating redox-sensitive transcription factors and causing inflammation and further enhancing the prevailing oxidative stress and continuing cyclic episodes that lead to disease establishment and progression.[13,15] Inhibition of AR blocks the production of GS-lipid alcohols which could halt this cycle and prevents disease progression.

References

1. Read R. Uveitis: advances in understanding of pathogenesis. *Curr Rheumatol Rep.* 2006;8:260–266.
2. Gritz DC, Wong IG. Incidence and prevalence of uveitis in Northern California; the Northern California Epidemiology of Uveitis Study. *Ophthalmology.* 2004;111:491–500.
3. Feuermannová A. Inflammatory diseases of the eye (in Czech). *Vnitr Lek.* 2007;53:521–523.
4. Smith JR. Management of uveitis. *Clin Exp Med.* 2004;4:21–29.
5. Yadav UC, Srivastava SK, Ramana KV. Understanding the role of aldose reductase in ocular inflammation. *Curr Mol Med.* 2010;10:540–549.
6. Muñoz-Fernández S, Martín-Mola E. Uveitis. *Best Pract Res Clin Rheumatol.* 2006;20:487–505.
7. Tabbara KF. Infectious uveitis: a review. *Arch Soc Esp Oftalmol.* 2000;75:215–259.
8. Smith JR, Hart PH, Williams KA. Basic pathogenic mechanisms operating in experimental models of acute anterior uveitis. *Immunol Cell Biol.* 1998;76:497–512.
9. Singh VK, Biswas S, Anand R, Agarwal SS. Experimental autoimmune uveitis as animal model for human posterior uveitis. *Indian J Med Res.* 1998;107:53–67.
10. Agarwal RK, Caspi RR. Rodent models of experimental autoimmune uveitis. *Methods Mol Med.* 2004;102:395–419.
11. Bodaghi B, Rao N. Relevance of animal models to human uveitis. *Ophthalmic Res.* 2008;40:200–202.
12. Caspi RR. A look at autoimmunity and inflammation in the eye. *J Clin Invest.* 2010;120:3073–3083.
13. Srivastava SK, Ramana KV, Bhatnagar A. Role of aldose reductase and oxidative damage in diabetes and the consequent potential for therapeutic options. *Endocr Rev.* 2005;26:380–392.
14. Alexiou P, Pegklidou K, Chatzopoulou M, Nicolaou I, Demopoulos VJ. Aldose reductase enzyme and its implication to major health problems of the 21st century. *Curr Med Chem.* 2009;16:734–752.
15. Ramana KV, Srivastava SK. Aldose reductase: a novel therapeutic target for inflammatory pathologies. *Int J Biochem Cell Biol.* 2010;42:17–20.
16. Yadav UC, Srivastava SK, Ramana KV. Aldose reductase inhibition prevents endotoxin-induced uveitis in rats. *Invest Ophthalmol Vis Sci.* 2007;48:4634–4642.
17. Hotta N, Toyota T, Matsuoka K, et al. Clinical efficacy of fidarestat, a novel aldose reductase inhibitor, for diabetic peripheral neuropathy: a 52-week multicenter placebo-controlled double-blind parallel group study. *Diabetes Care.* 2001;24:1776–1782.
18. Satici A, Guzey M, Gurler B, Vural H, Gurkan T. Malondialdehyde and antioxidant enzyme levels in the aqueous humor of rabbits in endotoxin-induced uveitis. *Eur J Ophthalmol.* 2003;13:779–783.
19. Wu GS, Zhang J, Rao NA. Peroxynitrite and oxidative damage in experimental autoimmune uveitis. *Invest Ophthalmol Vis Sci.* 1997;38:1333–1339.
20. Saraswathy S, Rao NA. Photoreceptor mitochondrial oxidative stress in experimental autoimmune uveitis. *Ophthalmic Res.* 2008;40:160–164.
21. Bosch-Morell F, Romá J, Puertas FJ, Marín N, Díaz-Llopis M, Romero FJ. Efficacy of the antioxidant ebselen in experimental uveitis. *Free Radic Biol Med.* 1999;27:388–391.
22. Yadav UC, Kalariya NM, Ramana KV. Emerging role of antioxidants in the protection of uveitis complications. *Curr Med Chem.* 2011;18:931–942.
23. Lin FY, Chen YH, Tasi JS, et al. Endotoxin induces toll-like receptor 4 expression in vascular smooth muscle cells via NADPH oxidase activation and mitogen-activated protein kinase signaling pathways. *Arterioscler Thromb Vasc Biol.* 2006;26:2630–2637.
24. Woo CH, Lim JH, Kim JH. Lipopolysaccharide induces matrix metalloproteinase-9 expression via a mitochondrial reactive oxygen species-p38 kinase-activator protein-1 pathway in Raw 264.7 cells. *J Immunol.* 2004;173:6973–6980.
25. Davey MP, Rosenbaum JT. The human leukocyte antigen complex and chronic ocular inflammatory disorders. *Am J Ophthalmol.* 2000;129:235–243.
26. Kerr EC, Copland DA, Dick AD, Nicholson LB. The dynamics of leukocyte infiltration in experimental autoimmune uveoretinitis. *Prog Retin Eye Res.* 2008;27:527–535.
27. Rajendram R, Saraswathy S, Rao NA. Photoreceptor mitochondrial oxidative stress in early experimental autoimmune uveoretinitis. *Br J Ophthalmol.* 2007;91:531–537.
28. Saraswathy S, Rao NA. Mitochondrial proteomics in experimental autoimmune uveitis oxidative stress. *Invest Ophthalmol Vis Sci.* 2009;50:5559–5566.
29. Srivastava S, Vladykovskaya E, Barski OA, et al. Aldose reductase protects against early atherosclerotic lesion formation in apolipoprotein E-null mice. *Circ Res.* 2009;105:793–802.
30. Hattori T, Matsubara A, Taniguchi K, Ogura Y. Aldose reductase inhibitor fidarestat attenuates leukocyte-endothelial interactions in experimental diabetic rat retina in vivo. *Curr Eye Res.* 2010;35:146–154.
31. Reddy AB, Srivastava SK, Ramana KV. Anti-inflammatory effect of aldose reductase inhibition in murine polymicrobial sepsis. *Cytokine.* 2009;48:170–176.
32. Ravindranath TM, Mong PY, Ananthakrishnan R et al. Novel role for aldose reductase in mediating acute inflammatory responses in the lung. *J Immunol.* 2009;183:8128–8137.
33. Tammali R, Ramana KV, Singhal SS, Awasthi S, Srivastava SK. Aldose reductase regulates growth factor-induced cyclooxygenase-2 expression and prostaglandin E2 production in human colon cancer cells. *Cancer Res.* 2006;66:9705–9713.
34. Tammali R, Ramana KV, Srivastava SK. Aldose reductase regulates TNF-alpha-induced PGE2 production in human colon cancer cells. *Cancer Lett.* 2007;252:299–306.
35. Yadav UC, Ramana KV, Aguilera-Aguirre L, Boldogh I, Boulares HA, Srivastava SK. Inhibition of aldose reductase prevents experimental allergic airway inflammation in mice. *PLoS One.* 2009;4:e6535.
36. Caspi RR. Experimental Autoimmune uveoretinitis in the rat and mouse. In: Coligan JE, ed. *Current Protocols in Immunology.* Hoboken, NJ: John Wiley & Sons, Inc.; 2003:Unit 15.6.1–15.6.20.
37. Amadi-Obi A, Yu CR, Liu X, et al. TH17 cells contribute to uveitis and scleritis and are expanded by IL-2 and inhibited by IL-27/STAT1. *Nat Med.* 2007;13:711–718.
38. Luger D, Caspi RR. New perspectives on effector mechanisms in uveitis. *Semin Immunopathol.* 2008;30:135–143.
39. Ho HT, Chung SK, Law JW, et al. Aldose reductase-deficient mice develop nephrogenic diabetes insipidus. *Mol Cell Biol.* 2000;20:5840–5846.
40. Shen DF, Chang MA, Matteson DM, Buggage R, Kozhich AT, Chan CC. Biphasic ocular inflammatory response to endotoxin-induced uveitis in the mouse. *Arch Ophthalmol.* 2000;118:521–527.

41. Rao NA, Romero JL, Fernandez MA, Sevanian A, Marak GE Jr. Role of free radicals in uveitis. *Surv Ophthalmol.* 1987;32:209–213.
42. Rao NA. Role of oxygen free radicals in retinal damage associated with experimental uveitis. *Trans Am Ophthalmol Soc.* 1990;88:797–850.
43. Caspi RR, Silver PB, Chan CC, et al. Genetic susceptibility to experimental autoimmune uveoretinitis in the rat is associated with an elevated Th1 response. *J Immunol.* 1996;157:2668–2675.
44. Foxman EF, Zhang M, Hurst SD, et al. Inflammatory mediators in uveitis: differential induction of cytokines and chemokines in Th1- versus Th2-mediated ocular inflammation. *J Immunol.* 2002;168:2483–2492.
45. Becker MD, Adamus G, Davey MP, Rosenbaum JT. The role of T cells in autoimmune uveitis. *Ocul Immunol Inflamm.* 2000;8:93–100.
46. Yang DD, Conze D, Whitmarsh AJ, et al. Differentiation of $CD4^+$ T cells to Th1 cells requires MAP kinase JNK2. *Immunity*. 1998;9:575–585.
47. Rincón M, Enslen H, Raingeaud J, et al. Interferon-gamma expression by Th1 effector T cells mediated by the p38 MAP kinase signaling pathway. *EMBO J.* 1998;17:2817–2829.